land

MDPI

Communication

A First Study of *Urginea maritima* Rings: A Case Study from Southern Jordan

Hezi Yizhaq [1,*], Abdel Rahman Mohammad Said Al-Tawaha [2] and Ilan Stavi [3,4]

[1] Department of Solar Energy and Environmental Physics, Blaustein Institutes for Desert Research, Ben-Gurion University of the Negev, Sede Boqer Campus 84990, Israel
[2] Department of Biological Sciences, Al Hussein Bin Talal University, Maan P.O. Box 20, Jordan; abdel.al-tawaha@mail.mcgill.ca
[3] Dead Sea and Arava Science Center, Yotvata 88820, Israel; istavi@adssc.org
[4] Eilat Campus, Ben Gurion University of the Negev, Eilat 88199, Israel
* Correspondence: yiyeh@bgu.ac.il; Tel.: +972-547-880-762

Abstract: Vegetation rings are a common pattern in water-limited environments and mostly occur in clonal plants. This study presents, for the first time, rings of the geophyte species *Urginea maritima*. The rings, typically 40–90 cm in diameter, are abundant in the sandy environment of Little Petra and Wadi Rum, in the southern Jordanian drylands. Soil properties were studied in the rings' center, periphery, and matrix. Soil-water volumetric content was significantly higher in the rings' periphery than in the center and matrix. The soil organic carbon was highest in the periphery, intermediate in the center, and lowest in the matrix. At the same time, the soil texture, hydraulic conductivity, and gravimetric moisture content at the hygroscopic level were similar in the three microenvironments. According to the results, a possible ring formation mechanism is the soil-water uptake mechanism, which results in competition between the plants at the periphery and those in the center and is generally attributed to plants with large lateral root zones. Numerical simulations of a mathematical model implemented in this study support the soil-water uptake mechanism. A second possible mechanism is negative plant-soil feedback due to the accumulation of dead biomass and its consequent decomposition, with the resultant release of autotoxic compounds. It is possible that several mechanisms occur simultaneously and synergistically affect the formation of *U. maritima* rings.

Keywords: central dieback; geophyte; soil-water content; vegetation ring; water uptake mechanism; plant-soil feedback

Citation: Yizhaq, H.; Al-Tawaha, A.R.M.S.; Stavi, I. A First Study of *Urginea maritima* Rings: A Case Study from Southern Jordan. *Land* **2022**, *11*, 285. https://doi.org/10.3390/land11020285

Academic Editor: Evan Kane

Received: 13 January 2022
Accepted: 11 February 2022
Published: 13 February 2022

1. Introduction

Vegetation rings are common in drylands. This pattern is usually found in clonal plants with confined lateral roots, growing in sandy soils. However, plant species with extended roots can also form rings. Depending on environmental conditions, such as slope incline or developmental stage [1], the ring-forming species may also create spot-like or crescent-like patterns. Recently, forb- and grass-forming rings were discovered in Namibian drylands and were termed "collective plant rings." Their formation mechanism is still unknown as no dieback has been observed in the center [2]. The soil-water content for these new rings was higher in the ring periphery than inside the ring, probably due to water depletion by the many grass individuals at the rim.

Four main mechanisms for clonal plants' ring formation were reviewed by Bonanomi et al. [3]: 1. Architectural constraints and the natural senescence of the clone's inner ramets [4,5]. 2. Physical disturbance caused by fire or droughts, e.g., [6]. 3. Competition for water between the ramets, which leads to central dieback. Two sub-mechanisms were proposed in this context (Figure 1). The first is the infiltration feedback that increases surface water flow towards the ring periphery. This feedback can be further enhanced by aeolian processes and biocrust growth in the patch's center and matrix [7–9]. For example, this mechanism

was proposed for rings of the *Asphodelus ramosus* L. in the drylands of Israel's Negev Desert [1,9–12]. The second mechanism, known as the water uptake mechanism, can form rings in plant species with large lateral root systems—for example, the creosote bush (*Larrea tridentata* (DC.) Coville), a xerophytic evergreen shrub species that dominates the arid southwestern United States [13]. 4. Negative plant-soil interactions, such as allelopathy or autotoxicity, which can be either direct, through the release of toxic materials, or mediated by microorganisms' phytotoxic activities, e.g., [14,15]. Recently, it was suggested that the large rings of the spinifex (*Triodia* spp.) tussock grass in Australia originate from a single old individual that expanded laterally over long time periods, whereby mechanisms such as microbial pathogens' effects in the plant's center cause dieback and induce the ring formation [16]. Notably, more than one mechanism may be simultaneously involved in forming the very same rings—e.g., soil-water uptake and negative plant-soil feedbacks—making the study of ring formation more complex as it is difficult to distinguish between the different processes.

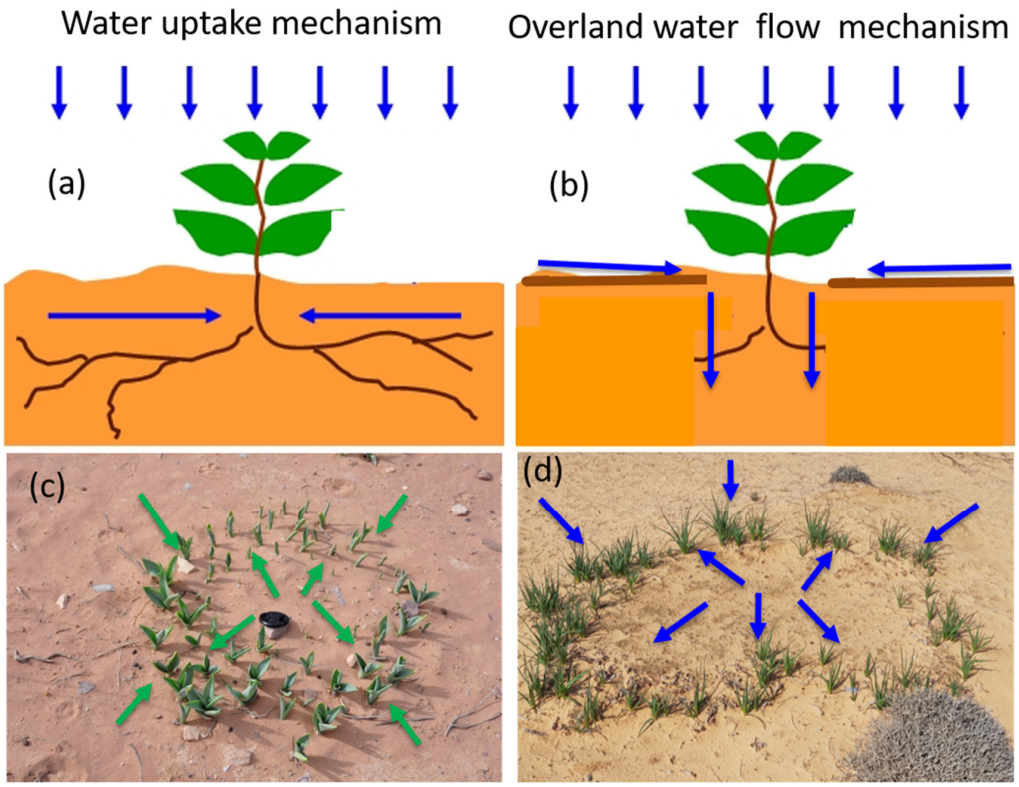

Figure 1. Schematic illustration of the two ring formation mechanisms that are dictated by water competition between individual plants. (**a**) The water uptake mechanism, which is related to the root augmentation feedback. Larger biomass leads to extended roots that can uptake soil water from a larger zone; illustrated by a *Urginea maritima* ring (**c**). (**b**) The overland flow mechanism, which is attributed to the infiltration contrast between the bare soil (often covered by biocrust) and the plant-covered soil (where biocrust growth is inhibited); illustrated by a *Asphodelus ramosus* ring (**d**). Surface water flows from the bare soil towards the plant-covered soil, where infiltration is higher. Both mechanisms can lead to ring formation from an expanded spot to in-phase distribution of biomass and soil water, i.e., the soil water is higher under the biomass and lower in the bare soil [11].

According to the vegetation pattern formation theory, rings are localized structures that lack spatial periodic patterns such as gaps or stripes [17]. A ring can be considered a large spot in which water is sufficient for the ramets in the periphery but not for the ramets in the center [1,9–11]. Deterministic mathematical models, based on the combination of short-range facilitation and long-range competition or inhibition, are used to describe vegetation pattern formation. The combination of short-range facilitation and long-range

competition can result in a finite-wavenumber instability (also known as Turing instability) of the uniform vegetation state and, thereby, of the formation of vegetation patterns such as gaps, labyrinths, stripes, and spots along the precipitation gradient [17,18].

In this work, we present a first study of *Urginea maritima* (L.) Baker (syn. *Drimia maritima* (L.) Stearn) rings, which are found in the drylands of southern Jordan and which cause the center dieback. The study's objective was to assess the mechanism behind the formation of *U. maritima* rings. The study's hypothesis was that ring formation is related to intraspecific competition for water between the ramets at the periphery and those at the center, which causes a central dieback and an outwardly expanding ring.

2. Materials and Methods

2.1. Regional Settings

Little Petra (Siq al-Barid) is located in an arid mountainous region in southern Jordan (30°22′20.04″ N, 35°26′48.13″ E, ~1040 m.a.s.l.; Figure 2). Average annual rainfall is about 85 mm, and the rainy season extends between October and March. The mean yearly temperature is 17.3 °C, with winter's minimum temperatures occasionally dropping below freezing and summer's maximum temperatures reaching ~40 °C.

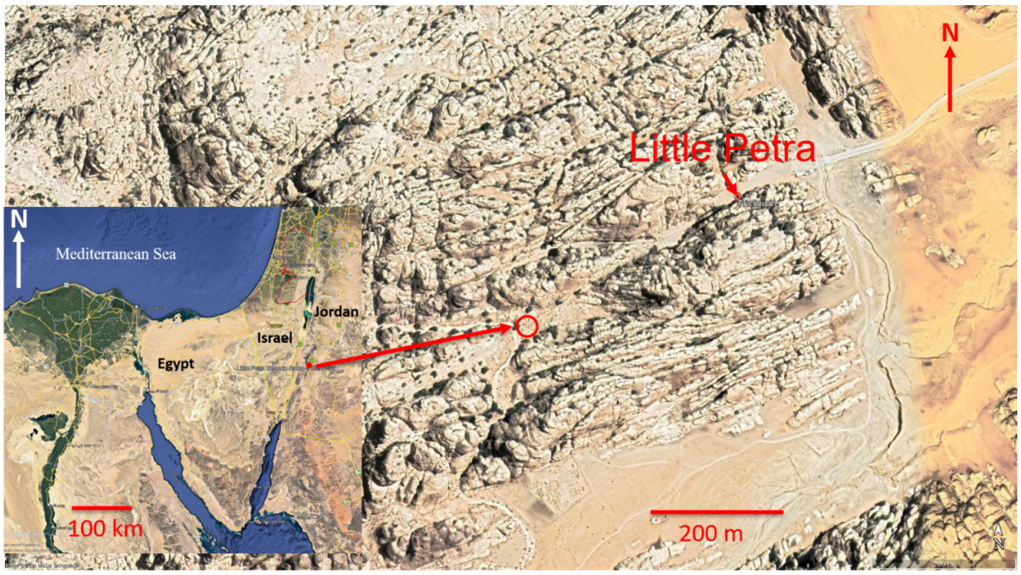

Figure 2. A regional map (lower left corner), with an extension of the study site, near Little Petra, Jordan. The topography is dominated by sandstone mountains and deep wadis between them. The study site is marked by a red circle.

Abundant rings of *U. maritima* exist across the region (Figures 2 and 3). *U. maritima* belongs to the Liliaceae family, grows in Mediterranean woodlands, shrublands, and steppe biomes [19], and has a unique life cycle. The plant produces a cluster of leaves in late autumn that remain until the end of spring. The leaves are basal, lanceolate to linear-lanceolate, glabrous, and with smooth margins. In the hot, dry months of May and June, the leaves dry up. In August, a tall flowering stem shoots up from the bulb, supporting flowers that bloom between late August and late October. The stem is 60–150 cm high, and its small white flowers extend from its midpoint upwards. The species is abundant in Israel and in southern Jordan, but interestingly and for yet unknown reasons, rings of *U. maritima* are very rare in Israel, whereas they are very common in southern Jordan. For example, *U. maritima* rings are also found in the hyper-arid, sandy region of Wadi Rum in far southern Jordan, where annual precipitation is approximately 50 mm/year.

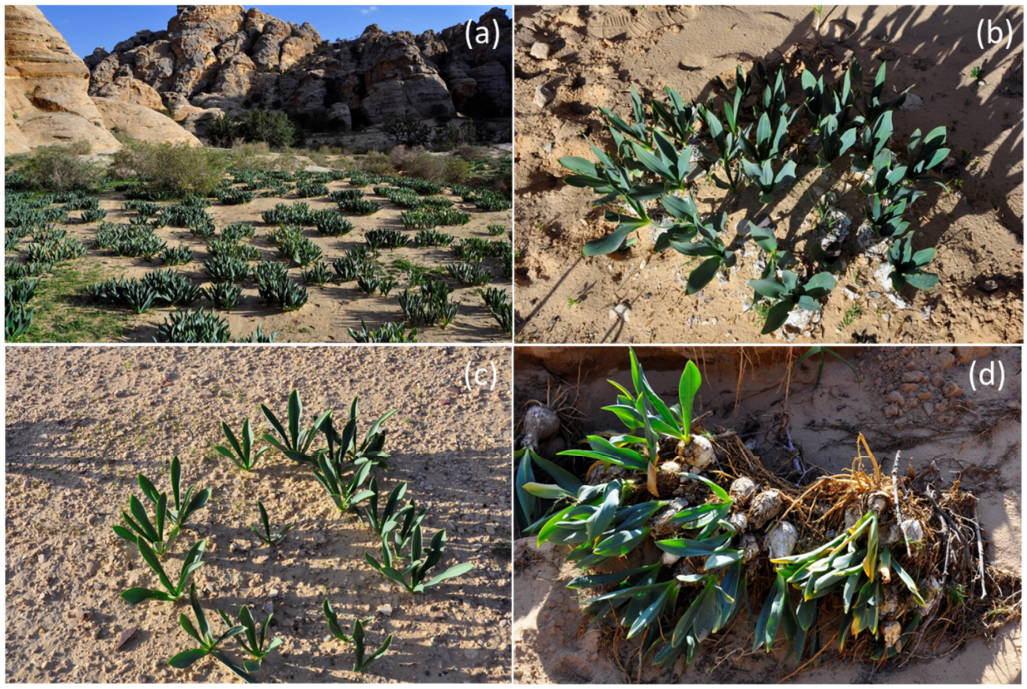

Figure 3. (**a**) A view of the study site, ca. 0.5 km south of Little Petra, southern Jordan. Two rings of *U. maritima* are shown in panels (**b**,**c**). Note that the plant in the middle of the ring in panel (**c**) is smaller than the plants in the ring's periphery, probably due to the intense competition over soil water with the plants in the periphery. (**d**) Bulbs of an *U. maritima* ring that were uprooted by a flooding stream. Note the long lateral roots that extend from the bulbs.

2.2. Field Measurements

Fieldwork was conducted in mid-March of 2014 and included detailed measurements and sampling of 15 *U. maritima* rings. Volumetric soil-water content, from three depths (7.5, 12, and 20 cm, which are the probe lengths), in three microenvironments (the ring's center, periphery, and matrix, Figure 4), and in five replicates per microenvironment, was measured by a time-domain reflectometer (TDR, HydroSense II, Campbell Scientific, Inc. Logan UT). We used a mini-disk infiltrometer (Decagon Devices, Pullman, WA, USA, 2007) to assess the unsaturated infiltration rate, in five replicates per microenvironment, for each of the 15 rings.

For each of the studied rings, five soil samples were obtained from the 3.5 and 7 cm depths in each micro-environment and taken to the laboratory for analysis. Gravimetric moisture content at the hygroscopic level was assessed by drying the samples to a constant weight at 105 °C for 24 h. The soil texture was assessed using the hydrometer method [20]. Soil organic matter (SOM) content (%) was determined by the dry combustion method [21]. The results were then divided by 1.724 to calculate soil organic carbon (SOC).

2.3. Mathematical Modeling

In the current study, we used the mathematical model introduced by Gilad et al. [22,23], which has been used in the context of ring formation in drylands [1,9–11], and here, we briefly describe its main assumptions. The model consists of a system of three nonlinear partial integro-differential equations for three dynamical variables that depend on space and time: (i) a biomass variable $b(\vec{r},t)$, representing the plants' aboveground biomass surface density, where the vector $\vec{r} = (x,y)$ represents the two spatial coordinates, and t represents time; (ii) a soil-water content variable, $w(\vec{r},t)$, describing the amount of soil water per unit area of the ground surface; and (iii) a surface water variable, $h(\vec{r},t)$, describing the height of a thin water layer above ground (more details of the model and the full description of the equations can be found in [9,10]).

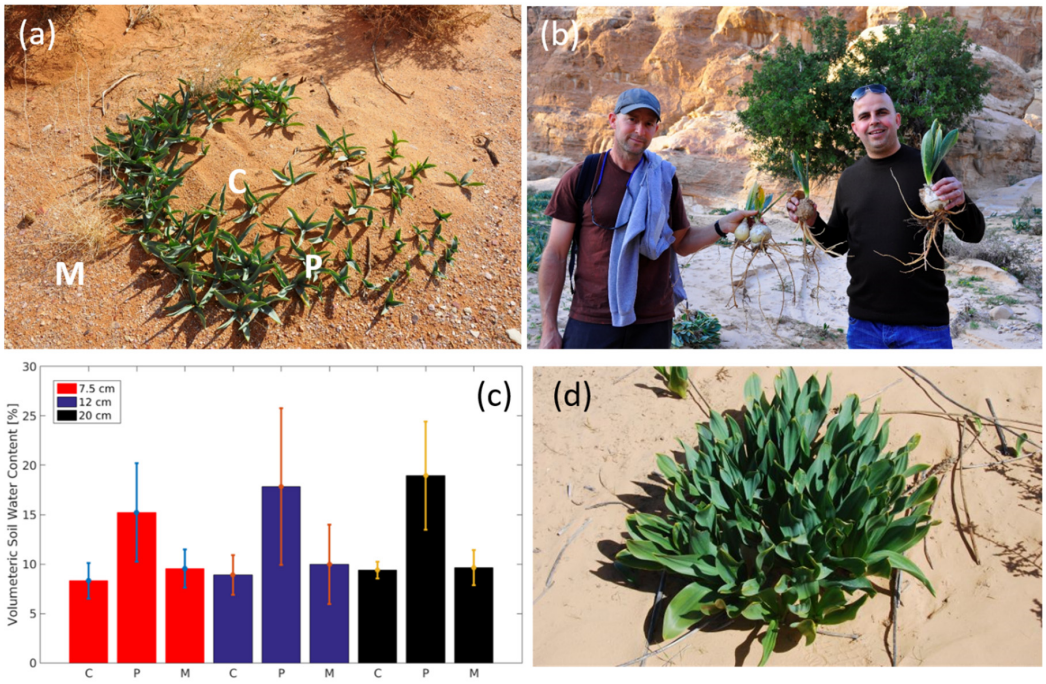

Figure 4. (**a**) A *U. maritima* ring indicating the three microenvironments: center (C), periphery (P), and matrix (M). (**b**) Two of the co-authors holding *U. maritima* plants that were uprooted and washed away by a flooding stream. Note the long and lateral roots of *U. maritima* (more than 30 cm in length). (**c**) Mean soil volumetric moisture content according to microenvironment and depth. (**d**) A spot of *U. maritima* growing on sand in the northern Negev Desert in Israel (mean annual precipitation is about 150 mm/year).

On a flat surface, two water-transport processes dictate the local amount of soil water in the model: (i) surface water flow from bare areas, including the bare inner circle, towards vegetation patches, due to higher infiltration rates in the vegetated areas [24]. This process is known as the infiltration feedback, and (ii) water uptake by plant roots that may extend far beyond the plant canopies, i.e., the root augmentation feedback that can be found in many plants in water-deprived environments. The infiltration feedback is dictated by a dimensionless parameter f that varies between zero and unity [23]. By using the parameter f, we can define the degree of the *infiltration contrast* (c) between vegetated and bare soil areas as $c = f^{-1} - 1 \geq 0$. Values of $c << 1$ ($f \cong 1$) imply low infiltration contrasts, whereas value $c \gg 1$ ($f << 1$) stands for high infiltration contrasts, occurring mostly when biological or physical soil crusts decrease the infiltration rate in bare soil (e.g., $f = 0.1$ was used by Yizhaq et al. [9] for modeling the infiltration feedback to explain the *Asphodelus ramosus* ring formation, whereas in this study, we used $f = 1$ which means no infiltration contrast). The water-uptake process is controlled by a root-augmentation parameter, η, that quantifies the rate extension of the root system L increases due to increase in the aboveground biomass increases: $\eta \propto dL/db$. The value $\eta = 0$ represents the root zone of fixed sizes, independent of the biomass. The rainfall rate, p, is very important in modeling vegetation in a water-limited system. This should generally be a time-dependent parameter to represent the temporal stochasticity in rainfall and to account for seasonal rainfall variations, as well as inter-annual variations. However, in this work, we neglected inter-annual rainfall variations and chose a simple representation for p to be time-periodic with an annual period consisting of an n-month rainy period followed by an m-month dry period with no rainfall, where $m + n = 12$. We chose $n = 4$ as the duration of the rainy period, typical to dry climate with strong seasonal variability (such as the Mediterranean climate). The choice of $n = 12$ represents climates with uniform precipitation rate with no seasonal variability, better-representing plants with large η values such as shrubs, and it

was studied by Sheffer et al. [11] for explaining ring formation of the perinatal shrub *Larrea tridentata* (Creosote bush).

The development of ring formation involves two main phases. The first is a latent-ring phase, in which the ring is not observable, but the biomass in the ring edges is greater than that in the core. In the second phase, the ring is visible, as the soil is bare in the core without biomass. To quantify the degree of the ring formation process from spot to a full ring, we introduce a ring index [10], where Δ is defined as

$$\Delta = (b_{\max} - b_{core})/b_{\max} \quad (1)$$

where $b_{\max}$ is the maximal biomass in the patch (for a ring it is the biomass at the peripery), and b_{core} is the biomass in the patch core (for a visible ring it will be zero). According to this definition, spots are represented by a zero-ring index, $\Delta = 0$, while visible rings with a bare center are characterized by $\Delta = 1$. Intermediate index values, $0 < \Delta < 1$, represent latent rings. Thus, during the temporal process of ring formation from an initial uniform spot to a visible ring, the ring index increases from zero to unity.

In the numerical simulations, we solve the model equations on spatial grids representing systems larger than the size of individual spots or rings. The simulation time corresponding to 50 years was chosen to ensure long-term ecological stability of the patterns. However, the model does not include any process that can slow down the expansion of a single ring. It is important to note that the model simulations presented in this work do not aim to model the specific *U. maritima* ring formations as the exact values of the parameters are not known, but the aim is to conduct a qualitative assessment of the main mechanism or process of *U. maritima* ring formation, and to qualitatively compare the soil-water distribution with field measurements. The description and the values of the parameters used in the simulations can be found in [9].

3. Results and Discussion

3.1. Soil-Water Content and Soil Analyses

The mean volumetric soil-water content results are shown in Figure 4c. For all depths, this soil property was significantly higher in the periphery than in the center and matrix, whereas the soil-water content in the matrix and center was similar.

The results of the soil analyses are detailed in Table 1. There was no significant difference in the content of clay (~9%), silt (~11%), or sand (~80%) among the three microenvironments. The only significant difference between depths was found for the very fine sand (53–106 μm) and the fine sand (106–250 μm) fractions, with greater mean values in the shallower depth than those in the deeper depth. The gravimetric soil moisture and hydraulic conductivity were similar in all microenvironments. At the same time, the SOC was significantly affected by microenvironment, and was highest in the periphery, intermediate in the center, and lowest in the matrix. The SOC trend is similar to that recorded for the *A. ramosus* rings in the drylands of Israel's Negev Desert [9,12].

3.2. Numerical Simulations

Overall, except for the difference in SOC, the results suggest that soil properties are similar in all microenvironments. Therefore, the infiltration feedback, or the water overland flow mechanism, which is based on a spatial redistribution of the surface water due to biocrust development or the deposition of fine particles in the ring's center with the consequent reduced water infiltrability [8], is probably not the mechanism that forms *U. maritima* rings. The second mechanism—the root-augmentation feedback, or the "water uptake mechanism," which characterizes plants with laterally extended root systems [11] —seems to be relevant for our case study. It is important to note that from the mathematical modeling approach, both mechanisms predict in-phase biomass and soil-water distribution. This means that the soil-water content is higher under the vegetation patch, which accords with the field measurements.

Table 1. (A) Microenvironment effect on the soil texture; (B) Depth effect on the soil texture; (C) Microenvironment effect on the soil gravimetric moisture content (SM), hydraulic conductivity (*K*), and organic carbon content (SOC).s.

A	53–106 µm (%)	106–250 µm (%)	250–500 µm (%)	500–1000 µm (%)	1000–2000 µm (%)
	very fine sand	fine sand	medium sand	coarse sand	very coarse sand
p value	0.2138	0.8849	0.213	0.3004	0.6751
Center	7.8 a (0.6)	39.2 a (1.2)	39.1 a (1.5)	2.2 a (0.1)	0.38 a (0.05)
Periphery	7.5 a (0.6)	39.4 a (0.9)	36.7 a (1.2)	2.1 a (0.2)	0.34 a (0.04)
Matrix	8.2 a (0.5)	38.7 a (1.0)	36.8 a (1.4)	1.9 a (0.2)	0.37 a (0.06)
B	53–106 µm (%)	106–250 µm (%)	250–500 µm (%)	500–1000 µm (%)	1000–2000 µm (%)
p value	**0.0295**	**0.0292**	0.8345	0.3055	0.5812
Shallow (3.5 cm)	8.2 a (0.5)	40.3 a (1.0)	37.7 a (1.1)	2.0 a (0.2)	0.35 a (0.04)
Deep (7.5 cm)	7.5 b (0.5)	37.9 b (0.7)	37.4 a (1.2)	2.1 a (0.1)	0.37 a (0.04)
C	Gravimetric SM (%)	*K* (cm s^{-1})	SOC (g kg^{-1})		
p value	0.2142	0.7498	**0.0047**		
Center	4.86 a (0.20)	0.00109 a (0.00016)	11.9 ab (0.6)		
Periphery	5.16 a (0.26)	0.00131 a (0.00028)	13.0 a (0.6)		
Matrix	4.68 a (0.25)	0.00110 a (0.00021)	10.6 b (0.4)		

Notes: Bold *p* value indicates a significant effect. Means within the same column followed by a different letter differ at the 0.05 probability level according to Tukey's HSD. Numbers within parentheses are standard error of the means.

Within this mechanism (as described in Section 2.3), water transport is controlled by the values of η that quantifies the extent to which the lateral extension of the root system length L increases as the biomass increases. Higher values of η enable water transport from a larger space around the plant throughout the extended root system. This mechanism can form rings without an infiltration contrast between the vegetated and bare soil. As the patch grows, the plants in the periphery uptake water from the patch center, where the competition for water becomes stronger, resulting in central dieback and ring formation, as shown in Figure 5 for $\eta = 2$ and $f = 1$. Figure 6 shows both mechanisms of ring formation under uniform vegetation. Under the water uptake mechanism with $\eta = 2$ and $f = 1$ (denoted in black), the ring development rate varies in time; it is slow at the beginning, but after a certain point, the growth becomes faster. The ring's growth rate under the overland water flow with $\eta = 0$ and $f = 0.1$ means a constant root length and a strong infiltration feedback (marked in blue in Figure 6), and it is almost constant in time. This difference in the ring's temporal growth that is predicted by the model simulations can be used in long duration studies as an indication for the underlying mechanism. Interestingly, the average annual biomass is larger in the "water uptake ring" than in the "overland water flow ring", whereas the trend in the radius size is the opposite. Thus, despite the fact that the ring with $\eta = 0$ and $f = 0.1$ has a larger radius, the ring with the extended root zone $\eta = 2$ and $f = 1$ has larger biomass, because the larger roots can generally support larger biomass.

Another possible mechanism, which was not studied in the current work but could be relevant for the toxic characteristics of the *U. maritima*, is the negative plant-soil feedback. In this mechanism, autotoxicity or pathogen accumulation in the center of the initial patch causes central dieback, resulting in ring formation as the plant grows toward toxin- or pathogen-free soil [16,25]. It is important to note that multiple mechanisms can take place simultaneously. Regardless of the formation mechanism, the ring pattern is an efficient

vegetation pattern in drylands, as it increases the access to soil water from a larger area, allowing the plants to increase their biomass. One way or another, more field studies are needed to assess alternative mechanisms for the formation of *U. maritima* rings.

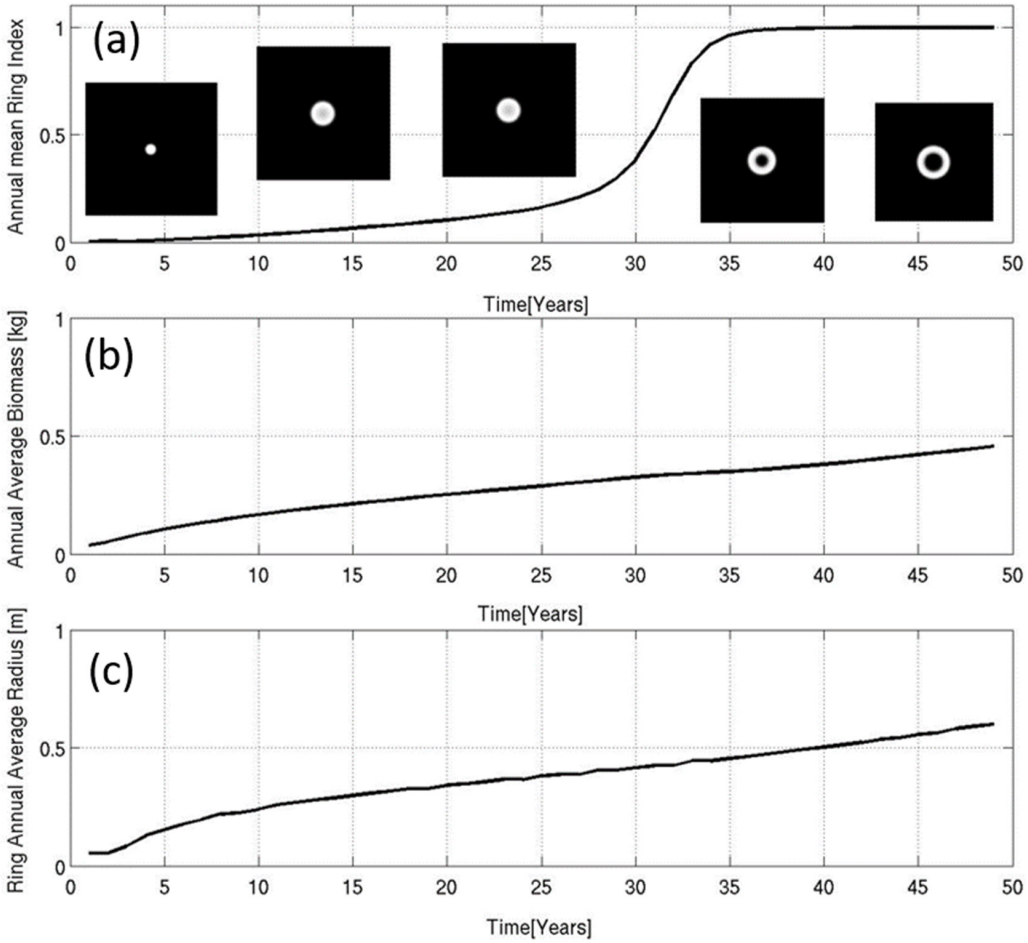

Figure 5. Model simulation of a ring formation due to the water uptake mechanism (see Sheffer et al., 2011) for 120 mm/year rainfall occurring in four months with $\eta = 2$ and $f = 1$, i.e., no infiltration contrast. (**a**) The evolution of the ring index defined as $\Delta = (\text{biomass}_{\text{periphery}} - \text{biomass}_{\text{center}})/\text{biomass}_{\text{center}}$; spots are characterized by $\Delta = 0$, and rings by $\Delta = 1$. The ring began as an initial small spot that expanded and, after 35 years, developed into a ring. (**b**) The average biomass increases over time but more rapidly after the ring formation. (**c**) The evolution of the ring's radius. Other parameter values can be found in [9,11]. Note that the parameters and the precipitation value used in these simulations are not specific to *U. maritima* but illustrate the ring formation due to the water uptake mechanism.

3.3. Biogeographic Implications

Clonal plant architecture [5] can be considered a necessary but insufficient condition for ring formation since a species that forms rings does not necessarily produce rings in a more humid condition. In areas that are more humid than southern Jordan (i.e., precipitation >80 mm/year), such as the northern Negev Desert in Israel (150 mm/year), *U. maritima* spots and rings are very rare. The rings expand more easily in sandy soil than in other soils, as was observed in the size of the *A. ramosus* rings in the Negev Desert in sandy and loess soils [12]. The ring pattern is an efficient form of clonal plant growth for improved survival in dryland ecosystems, where the dominant limiting factor is the access to water, which is unpredictable in space and time. In drylands, geophyte rings can develop through either mechanism. For example, *A. ramosus* rings develop due to the infiltration contrast between the bare soil and vegetation patches [9], whereas according to

our study, *U. maritima* rings develop due to the root augmentation feedback, which may be more efficient in drier environments, as the lateral roots can help the plants to extract water from a larger area. The average annual precipitation rate (98 mm/yr) in Coville in the Lucerne Valley, California, USA, where very large creosote bush rings exist, supports this hypothesis. However, more studies are needed to understand the link between the ring formation mechanism and climatic conditions.

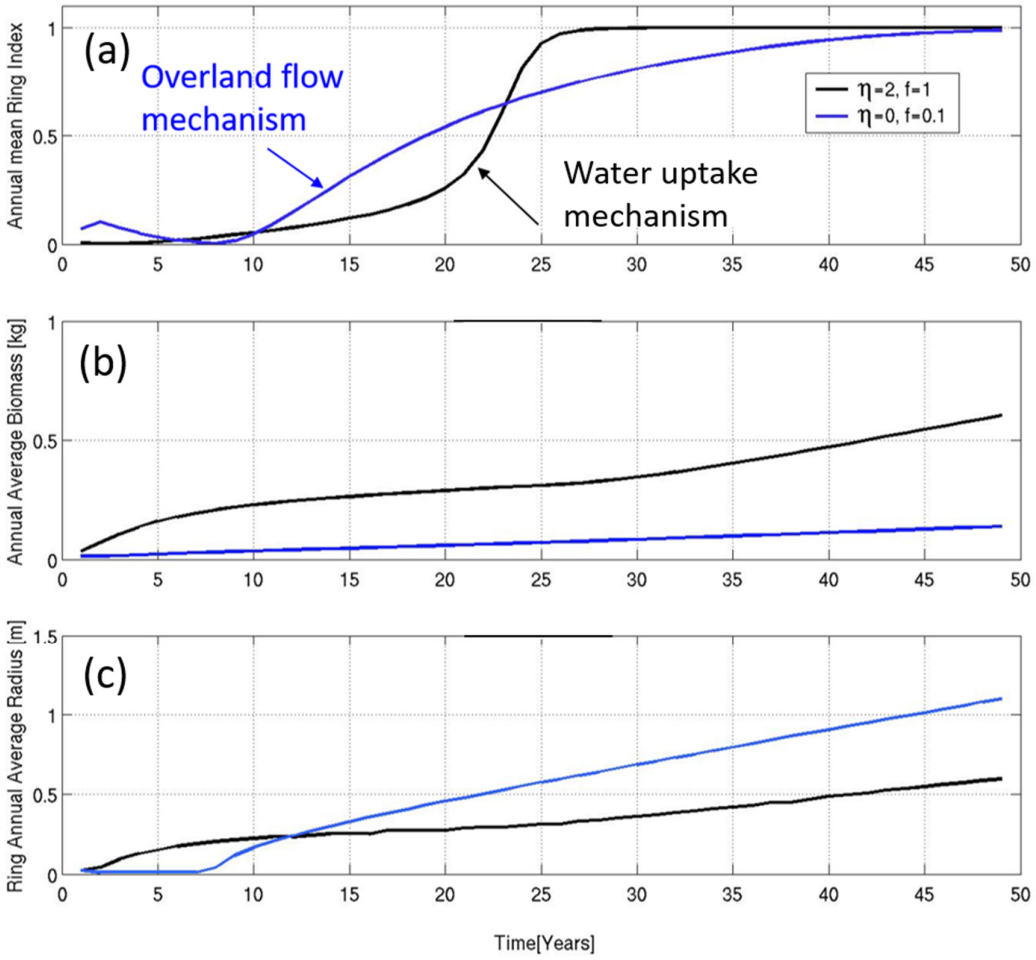

Figure 6. Model simulations of the two mechanisms for ring formation under uniform precipitation of 120 mm/year. The overland water flow mechanism (marked in blue) is characterized by $\eta = 0$ and $f = 0.1$, i.e., with a fixed root zone and a high infiltration feedback between the bare soil and vegetation patch. At the same time, the water uptake mechanism (marked in black) is characterized by $\eta = 2$ and $f = 1$, which means an extended root zone and no infiltration contrast. Ring index (**a**), average biomass (**b**), and average radius development (**c**) show the difference between the two mechanisms of ring formation. In the overland flow mechanism, the ring radius grows at a constant rate (after an initial phase during which it is constant), while in the water uptake mechanism, the ring growth rate varies in time.

Studies carried out at different soil depths similar to those studied in *U. maritima*, established that the areas with the highest growth points (meristems) in Musaceae bulb that gave rise to pseudostems, roots, and vegetative buds were influenced by soil texture, soil dry consistency, reaction to HCl, soil structure, and biological activity [26,27]. These studies may indicate that *U. maritima* could be influenced by the arid environment of sparse Mediterranean scrub or rocky terrain, with greater emphasis on the calcareous characteristics of the soil, which in the case of some plant species could affect the bulb and

subsequently the productivity, favoring the incidence of diseases in microenvironments, e.g., the ring's interior.

4. Conclusions

This study suggests that the *U. maritima* rings in the drylands of southern Jordan are formed due to the water uptake mechanism, which is attributed to the extended lateral roots of this geophyte species. The central dieback is induced by competition for water between the plants at the edges and those in the center. The soil-water content is higher in the ring edges than in the center. Our hypothesis is based on the soil analyses, which did not show any difference in the infiltration rate or the mechanical composition (texture) between the three microenvironments (ring center, periphery, and matrix), and is supported by numerical simulations of a well-studied mathematical model for vegetation in drylands with extended root systems and without an infiltration contrast.

Author Contributions: Field work and Methodology, H.Y., A.R.M.S.A.-T. and I.S.; numerical simulations, H.Y.; writing—original draft preparation, H.Y. and I.S. All authors have read and agreed to the published version of the manuscript.

Funding: This research received no external funding.

Data Availability Statement: The data is contained within this article.

Acknowledgments: We thank Ehud Meron for the fruitful discussions, which substantially improved the manuscript. The Dead Sea and Arava Science Center is supported by the Israel Ministry of Science and Technology. Also, the authors thank two anonymous reviewers, whose comments allowed the substantial improvement of the manuscript's original version.

Conflicts of Interest: The authors declare no conflict of interest.

References

1. Meron, E.; Yizhaq, H.; Gilad, E. Localized structures in dryland vegetation: Forms and functions. *Chaos* **2007**, *17*, 037109.1–037109.9. [CrossRef]
2. Getzin, S.; Yizhaq, H.; Tschinkel, W. Definition of "fairy circles" and how they differ from other common vegetation gaps and plant rings. *J. Veg. Sci.* **2021**, *32*, e13092. [CrossRef]
3. Bonanomi, G.; Incerti, G.; Stinca, A.; Cartenì, F.; Giannino, F.; Mazzoleni, S. Ring formation in clonal plants. *Community Ecol.* **2014**, *15*, 77–86. [CrossRef]
4. Danin, A.; Orshan, G. Circular arrangement of Stipagrostis ciliate clumps in the Negev, Israel and near Goakeb, Namibia. *J. Arid. Environ.* **1995**, *30*, 301–313. [CrossRef]
5. Danin, A. *Plants of Desert Dunes*; Springer: Berlin, Germany, 1996.
6. Adachi, N.; Terashima, I.; Takahashi, M. Central dieback of monoclonal stands of Reynoutria japónica in an early stage of primary succession on Mount Fuji. *Ann. Bot.* **1996**, *77*, 477–486. [CrossRef]
7. Ravi, S.; D'Odorico, P.; Okin, G.S. Hydrologic and aeolian controls on vegetation patterns in arid landscapes. *Geophys. Res. Lett.* **2007**, *34*, L24S23. [CrossRef]
8. Ravi, S.; D'Odorico, P.; Wang, L.; Collins, S. Form and function of grass ring patterns in arid grasslands: The role of abiotic controls. *Oecologia* **2008**, *158*, 545–555. [CrossRef]
9. Yizhaq, H.; Stavi, I.; Swet, N.; Zaady, E.; Katra, I. Vegetation ring formation by water overland flow in water-limited environments: Field measurements and mathematical modelling. *Ecohydrology* **2019**, *12*, e2135. [CrossRef]
10. Sheffer, E.; Yizhaq, H.; Gilad, E.; Shachak, M.; Meron, E. Why do plants in resource deprived environments form rings? *Ecol. Complex.* **2007**, *4*, 192–200. [CrossRef]
11. Sheffer, E.; Yizhaq, H.; Shachak, M.; Meron, E. Mechanisms of vegetation-ring formation in water-limited systems. *J. Theor. Biol.* **2011**, *273*, 138–146. [CrossRef]
12. Herooty, Y.; Bar, P.; Yizhaq, H.; Katz, O. Soil hydraulic properties and water source-sink relations affect plant rings' formation and sizes under arid conditions. *Flora* **2020**, *270*, 151664. [CrossRef]
13. Vasek, F.C. Creosote bush: Long-lived clones in the Mojave Desert. *Am. J. Bot.* **1980**, *67*, 246–255. [CrossRef]
14. Cartení, F.; Marasco, A.; Bonanomi, G.; Mazzoleni, S.; Rietkerk, M.; Giannino, F. Negative plant soil feedback and ring formation in clonal plants. *J. Theor. Biol.* **2012**, *313*, 153–161. [CrossRef] [PubMed]
15. Inderjit; Callaway, R.M.; Meron, E. Belowground feedbacks as drivers of spatial self-organizationand community assembly. *Phys. Life Rev.* **2021**, *38*, 1–24. [CrossRef] [PubMed]
16. Ross, N.D.; Moles, A.T. The contribution of pathogenic soil microbes to ring formation in an iconic Australian arid grass, *Triodia basedowii* (Poaceae). *Aust. J. Bot.* **2021**, *69*, 113–120. [CrossRef]

17. Meron, E. *Nonlinear Physics of Ecosystems*; Taylor and Francis: Abingdon, UK, 2015.
18. Maestre, F.T.; Benito, B.; Berdugo, M.; Concostrina-Zubiri, L.; Delgado-Baquerizo, M.; Eldridge, D.J.; Guirado, E.; Gross, N.; Kéfi, S.; Le Bagousse-Pinguet, Y.; et al. Biogeography of global drylands. *New Phytol.* **2021**, *231*, 540–558. [CrossRef]
19. Mitrakos, K.; Price, L.; Tzanni, H. The growth pattern of the flowering shoot of *Urginea Marituma* L. (Liliaceae). *Am. J. Bot.* **1974**, *61*, 920–924. [CrossRef]
20. Bouyoucos, G.J. Hydrometer method improved for making particle size analyses of soils. *Agron. J.* **1962**, *54*, 464–465. [CrossRef]
21. Nelson, D.W.; Sommers, L.E. Total carbon, organic carbon, and organic matter. In *Methods of Soil Analysis (Part 2). Madison*; Page, A.L., Ed.; American Society of Agronomy: Madison, WI, USA, 1996; pp. 961–1010.
22. Gilad, E.; von Hardenberg, J.; Provenzale, A.; Shachak, M.; Meron, E. Ecosystem engineers: From pattern formation to habitat creation. *Phys. Rev. Lett.* **2004**, *93*, 098105. [CrossRef]
23. Gilad, E.; von Hardenberg, J.; Provenzale, A.; Shachak, M.; Meron, E. A mathematical model of plants as ecosystem engineers. *J. Theor. Biol.* **2007**, *244*, 680–691. [CrossRef]
24. Eldridge, D.J.; Zaady, E.; Shachak, M. Infiltration through three contrasting biological soil crusts in patterned landscapes in the Negev, Israel. *Catena* **2000**, *40*, 323–336. [CrossRef]
25. Carlton, L.; Duncritts, N.C.; Anny Chung, Y.; Rudgers, J.A. Plant–microbe interactions as a cause of ring formation in *Bouteloua gracilis*. *J. Arid. Environ.* **2018**, *152*, 1–5. [CrossRef]
26. Olivares, B.O.; Calero, J.; Rey, J.C.; Lobo, D.; Landa, B.B.; Gómez, J.A. Correlation of banana productivity levels and soil morphological properties using regularized optimal scaling regression. *Catena* **2022**, *208*, 105718. [CrossRef]
27. Campos, O.; Araya-Alman, M.; Acevedo-Opazo, C.; Cañete-Salinas, P.; Rey, J.C.; Lobo, D.; Landa, B. Relationship between soil properties and banana productivity in the two main cultivation areas in Venezuela. *J. Soil Sci. Plant Nutr.* **2020**, *20*, 2512–2524. [CrossRef]